Effect of precursor concentration on zinc sulphide nanomaterial prepared by co-precipitation method

Veena Choudapur[1], A. B. Raju[2], Arvind Bennal[1]*

[1]*Department of Physics, KLE Technological University, Vidyanagar, Hubballi, 580 031, India*
[2]*Department of Electrical and Electronics Engineering, KLE Technological University, Vidyanagar, Hubballi 580 031, India*

*Corresponding author; Tel: (+91)9449187918; Fax: (+91) 8362374985; E-mail: arvindbennal@bvb.edu

Received: 31 March 2016, Revised: 04 October 2016 and Accepted: 10 November 2016

DOI: 10.5185/amp.2017/781
www.vbripress.com/amp

Abstract

The studies on luminescent II-VI semiconducting nanomaterials have attracted widespread attention, due to their potential applications in optoelectronic and biophotonic devices. Amongst II-VI group semiconductor nanoparticles, ZnS Nano Particles with large exciton binding energy and wide direct bandgap at room temperature have drawn considerable attention for exploring its interesting optoelectronic properties. In this paper, high band gap Zinc Sulphide nanocrystals are prepared by simple Co-precipitation method at different concentrations of precursors, and the role of sulphur concentration on structural and optical properties is studied. The Zinc Sulphide nanomaterial was prepared using low cost precursors and de ionised water as solvent without using any capping agents. As synthesized Zinc Sulphide nanocrystals were characterized by using X-ray diffraction (XRD), Energy Dispersive Spectroscopy analysis, UV-Visible Spectrophotometry, Photoluminescence, Scanning electron Microscopy (SEM) and Ellipsometry. X-ray diffraction studies revealed that as prepared of ZnS nanocrystals are Polycrystalline with Cubic phase with preferential orientation along (111) direction. The crystallite size of the order of 5-11nm were obtained. EDAX pattern confirms the presence of Zinc and Sulfur. From optical absorption measurements, it has been observed that the direct optical band gap energy increases from 4.4 to 5.2eV with decrease in sulphur concentration in ZnS and exhibit large quantum confinement effect. Ellipsometry was carried out to measure optical constants of ZnS thin film. The electrical conductivity of the film is measured for the film coated on ITO glass by two probe methods.

Keywords: ZnS thin film, high band gap, low cost precursors, spin coating, preheating.

Introduction

Nanoparticles of various semiconducting materials have been extensively investigated due to their interesting size-dependent optoelectronic properties. Nanostructured materials are the materials, having dimensions in the 1–100 nm range, which provide the greatest potentials for improving performance and extended capabilities of products in a number of applications **[1]**. Semiconducting nano materials belonging to II–VI, III-V and IV-VI group elements play an indispensable role in contemporary nanoelectronics. II-VI group semiconductors (Zinc and Cadmium chalcogenides) are wide band gap semiconductors and transparent conductors have significantly contributed to thin film devices. Wide-band gap materials in contrast typically have band gaps of the order of 2 to 4 eV. Wide-bandgap semiconductors are materials that permit devices to operate at much higher voltages, frequencies and temperatures than conventional semiconductor materials like silicon and gallium arsenide. The high temperature tolerance means that these devices can be operated at much higher power levels under normal conditions. They exhibit a significant quantum confinement effect; this quantum confinement effect can be utilized in controlling the particle size and optical band gap so as to control the optoelectronic properties. The optoelectronic properties of a nano semiconductor mainly depend on the crystallite size, morphology and their optical response which can be widely tuned through chemical synthesis methods of nanomaterials by varying the reaction conditions like precursor concentrations, pH, temperature, and time of reactions and by using various types of capping agents during synthesis in case of chemical methods **[1-4].**

Transparent Conductors (TCs) play a critical role in many current and emerging optoelectronic devices. These transparent conductors have generated great fundamental and technical interest in recent years due to their exceptional combination of high electrical conductivity and good optical transparency in the visible region of the

spectrum. TCs have been used in several fields such as flat panel displays, photovoltaic cells, low emissivity windows, electrochromic devices, chemical/biological sensors and transparent electronics. As a result, these II-VI semiconducting materials has been looked as a better choice for many potential applications including thin film solar cells, light-emitting diodes (LEDs), electroluminescence devices, flat panel displays, infrared windows, sensors, lasers, and bio devices, etc **[3,4].**

For the last few years, there has been growing interest in ZnS thin films due to their interesting optoelectronic properties. Zinc Sulphide is a very attractive semiconductor material due to its nontoxic nature, low cost starting materials, high refractive index (2.4), high direct optical band gap and high exciton binding energy of 40meV with n-type conductivity. ZnS crystallizes in cubic phase (E_g ~3.72 eV) and with hexagonal phase (E_g ~3.77 eV) and possesses transparency over wide range of solar spectrum **[1].** ZnS attract scientific interest due to the demand for non –toxic nanoparticulate semiconductor materials, which would reduce the amount of pollutants such as Cd, Hg, Pb released into the environment **[2]**. It can be used, as an antireflection coating or a window layer in thin film heterojuction solar cells. The primary function of a window layer in a heterojunction is to form a junction with the absorber layer while admitting a maximum amount of light to the junction region and absorber layer; no photocurrent generation occurs in the window layer. For high optical throughput with minimal resistive loss the bandgap of the window layer should be as high as possible and as thin as possible to maintain low series resistance **[4]**. It can be used as a reflector and dielectric filter in optics due to its high refractive index and transmittance in the visible range**.** Besides, it is abundant, highly stable, and environmentally friendly material, so that they are amenable also for biomedical applications **[1]**. Their wide band gaps make them ideal choice as inorganic passivation shells for a variety of semiconductor core/shell nanocrystals in order to improve the stability and emission properties of semiconductor core nanocrystals with relatively narrow band gaps. These wide-band-gap semiconductor nanocrystals are also attractive hosts for the formation of doped nanocrystals **[3]**. In recent years the development is taking place to develop Cd-free buffer layers for $CuInS_2$ and $Cu(In,Ga)Se_2$-based thin-film solar cells and modules. Thin films based on ZnS, ZnSe, ZnO, (Zn,Mg)O, $In(OH)_3$, In_2S_3, In_2Se_3 and $InZnSe_x$ were deposited on differently processed absorbers and tested as an alternative to the traditional CdS buffer which is toxic and not environment friendly. ZnS has a wider energy band gap than CdS, which results in the transmission of more high-energy photons to the junction, and to the enhancement of the blue response of the photovoltaic cells. Hence ZnS-based buffer layer is one of the most low cost and non toxic candidate for replacing the Chemical Bath Deposition (CBD) CdS for CIGS-based solar cells. **[3,4].** With these interests, various methods have been developed to grow ZnS nanomaterials, Silar method**[5]**,Chemical bath deposition **[6,11],** Co-precipitation method **[7],** sol gel method [**8,9],** thermal evaporation**[10],** Sputtering **[12],** etc. Among these Co-precipitation method of synthesis and deposition using spin coating has been considered as one of the cost effective deposition techniques **[13].**

In the present investigation ZnS nanomaterials of high band gap have been prepared by simple co-precipitation method.The effect of sulphur concentration on structural and optical properties were studied. The band gap decreases and the particle size increase with increase in sulphur concentration in ZnS. The enhancement of these properties is essential to develop the material as good candidate for a window layer, antireflection layer and buffer layer for low cost thin film solar cells.

Experimental

Materials

Zinc acetate [$Zn(OOCCH_3)_2$] of LR grade, Sodium sulphide flakes purified [Na_2S] of AR grade from sd-fine chem limited-India, were used as precursors for Zinc and Sulphur sources respectively. De ionized water is used as solvent and all the chemicals were used without further purification. ZnS NCs are synthesized at RT in aqueous medium at different precursor concentrations by simple co-precipitation method, using zinc acetate and sodium sulphide as precursors.

Method

Firstly 0.5M of Zinc acetate is prepared using de ionized water and is kept for continuous stirring. Another stock solution 0.5M sodium sulphide is prepared using de ionized water. The sodium sulphide solution is added to zinc acetate solution drop by drop with continuous stirring of 1000rpm on magnetic stirrer with temperature controlled at 60^0C. The pH of the solution is between 5 to 6. The reaction is carried out at 60^0C for 1hr in open conditions.

A white precipitate of ZnS nanocrystals is formed. The obtained precipitate was washed repeatedly by alternative ultrasonication and centrifugation using the solvent. Finally the precipitate was separated and dried at room temperature. Samples S1, S2 and S3 were prepared at different molar ratios of Zn^{+2}:S^{2-} as per **Table 1**. Prior to deposition of thin films, the glass slides were cleaned by standard procedure. First it was cleaned with soap solution then boiled in soap solution for 30 minutes and finally rinsed with copious amount of distilled water, followed by sonication in water for 10 minutes. Thin films of the obtained material were deposited using spin coating unit with 2000rpm for 30 sec. The as-deposited films were then pre-heated at 50°C for 5 minutes to evaporate the solvent and to remove organic residuals and again spin coated with2000rpm for 30 sec. This spinning to preheating procedure was repeated eight times.

Table 1. Experimental details of synthesis.

Sample	Chemicals used	Molar Conc Zn/S	Reaction conditions	pH
S1	zinc acetate, Na_2S and water	0.5M/0.5M	1000rpm, 60^0C for 1hr	5-6
S2	zinc acetate, Na_2S and water	0.5M/0.75M	1000rpm, 60^0C for 1hr	5-6
S3	zinc acetate, Na_2S and water	0.5M/1M	1000rpm, 60^0C for 1hr	5-6

Attempts were made to deposit films of all the samples at different speeds of spin coating at room temperature. On all deposits of ZnS thin films, the films that showed a good quality and uniform deposit were at the Zn/S ratio of 0.5M/0.5M. Therefore, this particular film was coated on both glass slides and indium tin oxide (ITO) glass slides for studies on electrical properties.

The Crystallanity of the samples was studied using X-ray diffractometer (Bruker AXS D8 Advance, STIC Cochin) operating at 1.5406A^{o}with CuKα radiation (1.5406A^0). UV-Visible Absorption measurements were performed in the wavelength range 200-800nm using UV-Vis-NIR Spectrophotometer V-670 Jasco International, Photoluminescence measurements were made using Fluorescence spectrophotometer Hitachi, Japan, The SEM image from STIC, Cochin, the EDS analysis form CeNSE-IISc Bangalore, the film optical constants were measured using an Ellipsometer M-2000U. J.A.Woollam Co. Inc. Bruker. The current-voltage curves were recorded on films using Keithley 617 programmable electrometer at room temperature.

Results and discussion

X-ray diffraction studies

Fig.1 shows the X-ray diffraction (XRD) spectra of the as prepared nano crystals measured in the scanning range 0-90^0. Phase identification was carried out with help of standard JCPDS No. 05-0566 data base. Three diffraction peaks are broadened and appeared with 2θ values of 28.740^0, 48.050^0, 56.460^0 corresponded to (111), (220) and (311) planes of cubic crystalline ZnS, respectively. This indicates that the prepared nano crystals are polycrystalline with preferential orientation along (111) direction and belong to the Cubic Zinc blende structure.

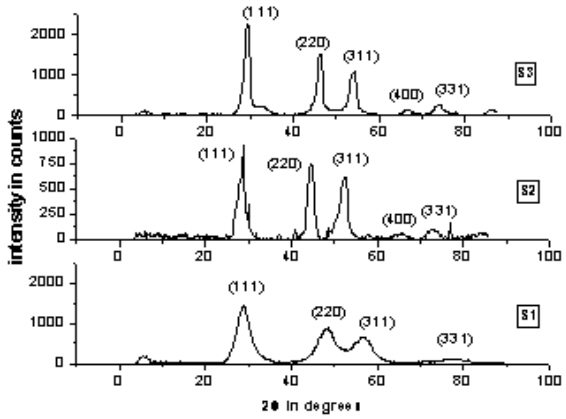

Fig. 1. XRD patterns of S1, S2, S3 samples.

Table 2. Lattice constants calculated from XRD pattern.

Peak 2θ in deg			(hkl)	'd' in A° obtained			'd' in A° Standard	Lattice Parameter α in A^0
S1	**S2**	**S3**		**S1**	**S2**	**S3**		
28.8	28.5	28.5	(111)	3.103	3.123	3.12	3.117	5.37
48.0	47.2	47.56	(220)	1.891	1.92	1.91	1.909	5.37
56.9	56.1	56.4	(311)	1.617	1.63	1.62	1.628	5.37

The lattice constant of the ZnS crystallites was determined from the XRD patterns using the formula

$$d_{hkl} = \frac{a}{\sqrt{h^2+k^2+l^2}}$$

The lattice parameter is computed as 5.37A^0 which is very close to standard value 5.42A^0. The XRD peaks are broadened due to nanocrystalline nature of as prepared sample. The crystallite size is calculated from the Debye Scherer equation [**14**],

$$D = \frac{0.94\lambda}{\beta\cos\theta}$$

where D is the average crystallite size, λ is the X-ray wavelength of Cu Kα radiation of value λ = 0.1506nm, θ is the diffraction angle and β is full width at half maximum (FWHM) of diffraction lines. The crystallite size were determined from the (111) line centered at 2θ = 28.74^0. The dislocation density (δ), which represents the amount of defects in the crystal, is calculated using the equation δ =1/D^2 and strain (ε) of the film is calculated using the equation ε = βcosθ/4 [**14**].

The structural parameters are calculated and presented in **Table 3.**

Table 3. Structural parameters.

Sample	Plane	d in A^0	FWHM(β) in radians	2θ^0	D in nm	δ in (nm)$^{-2}$	Strain 'ε'
S1	(111)	3.103	0.03	28.8	4.92	4.13x10^{-2}	0.726x10^{-2}
S2	(111)	3.123	0.017	28.55	8.56	1.36x10^{-2}	0.422x10^{-2}
S3	(111)	3.12	0.01354	28.578	11	0.826x10^{-2}	0.328x10^{-2}

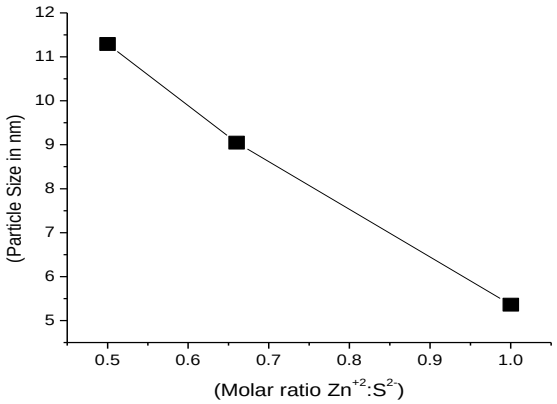

Fig 2. Graph of molar ratio Vs particle size.

It indicated that higher the Zn^{+2}:S^{2-} molar ratio, smaller is the particle size as in **Fig. 2**, the particle size as a function of precursor concentrations. It is observed that the particle size is dependent on the precursor concentrations. As the sulphur concentration increases the crystallanity and the crystallite size of the nanostructured

Zinc Sulphide increases. That is the amount of metal ions precipitated from solution increased with a decrease in the metal to sulphide ratio. At the higher concentrations, the nanoparticles formed are more in number and the particle size is larger due to availability of Zn^{+2} and S^{2-} ions. Since metal sulphides have low solubility and the high affinity between the reactants, metal sulphide precipitation reactions are inherently driven by high levels of supersaturation. As a result, metal sulphide precipitation reactions are difficult to control and a large number of small particles are formed during the process and therefore the amount of metal ions precipitated from solution increased with a decrease in the metal to sulphide ratio, that is percentage conversion of zinc ions increases with decrease in metal sulphide ratio resulting to the increase in the particle sizes. Theoretically from the metal sulphide precipitation kinetics, due to high metal removal and low solubility of the resulting metal precipitate the quantum yield is often lower. The number of zinc sulphide particles produced when excess sulphide was used to precipitate zinc ions from solution was very high compared to the case where stichiometric or lower sulphide concentrations was used. Thus, the results show, by changing the molar ratio, the particle size can be controlled [**15**]. The particle size can also be controlled by changing the pH of the reaction mixture as reported by Arup Kanti et al, there is an increase in the particle size from 1.2 to 1.5nm with increase in pH of the solution from 4 to 12 resulting large quantum confinement effect. Here also the ZnS nanocrystals were prepared in methenol medium and low cost precursor solutions were used without using any capping agent [**13**]. The Tran Thi et al reported the synthesis of Zinc Sulphide nanocrystals by hydrothermal method and obtained nanocrystals of 13.08nm, 14.57nm and 28.06nm at different precursor concentrations of 1:0.7, 1:1 and 1: 1.3 using zinc sulphate and Sodium sulphide as starting materials at 220^0C without using any capping agent [**16**]. The particle sizes of 25.57, 22.74 and 34.08 nm, respectively were reported in Ref. [**17**] at different annealing temparature of films of 300°C, 400°C and 500°C prepared by magnetron sputtering method. It has been observed that smaller particle sizes are obtained in chemical route methods than in physical methods.

In case nanocrystals prepared without using capping agent allows us to measure electrical conductivity easily whereas in case of nanocrystals which are prepared by using high cost and toxic capping molecules which are used to control the growth of the nanoparticles such as organic stabilizers may not allow to conduct current completely. In this work, even though the particles are formed of 5 to 11nm size, do not have much stability due to agglomeration of the particles as compared to colloidal solutions but to some extent agglomeration of particles can be minimized by longer time ultrasonication of nanoparticles dispersed in solvent and when spin coated, one can develop very thin films. Hence by controlling the particle size, viscosity and spin speed the thickness of the film can be varied.

Energy dispersive x-ray analysis

It is an analytical technique used for the elemental analysis or chemical characterization of a sample. It relies on an interaction of some source of X-ray excitation and a sample. The fundamental principle is that each element has a unique atomic structure allowing unique set of peaks on its X-ray emission spectrum. Interaction of an electron beam with a sample target produces a variety of emissions, including x-rays. An energy-dispersive (EDAX) detector is used to separate the characteristic x-rays of different elements into an energy spectrum and EDAX system software is used to analyze the energy spectrum in order to determine the abundance of specific elements. EDS can be used to find the chemical composition of materials down to a spot size of a few microns, and to create element composition maps over a much broader raster area. Together, these capabilities provide fundamental compositional information for a wide variety of materials.

In **Fig. 3** the EDAX spectrum compositional analysis is presented. The spectra show prominent peaks of Zn and S, and very small peaks of O, C. Elemental analysis shows there is a sulfur deficiency in the compositions of ZnS. A smaller value may due to a reaction of some 'S' ions with air during the reaction. This sulphur ion deficiency for ZnS thin film is also reported in ref. **[9]** due to surface oxidation of films exposed to air. The spectra show prominent peaks of Zn and S, and very small peaks of O, C and Na. The peaks of impurities O, C and Na may originate, respectively from the air atmosphere and the unreacted precursors. Also carbon contamination may be due to carbon tape used while performing EDS analysis. The results of XRD were further confirmed which showed that ZnS nanoparticles were of high purity.

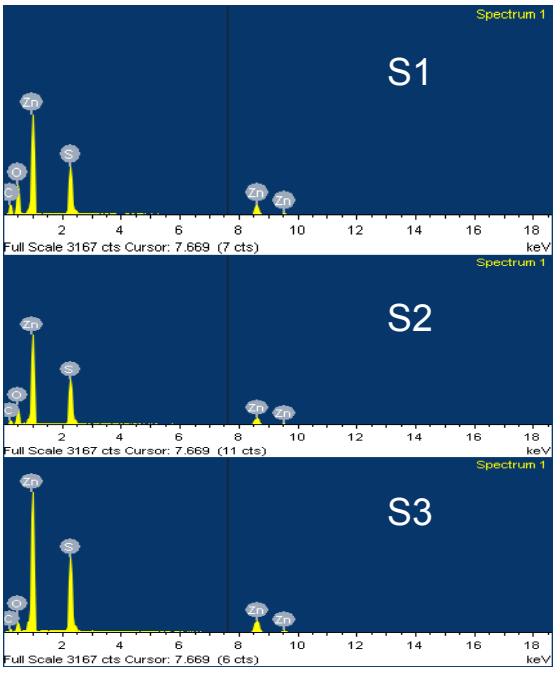

Fig 3. EDS graphs S1, S2, and S3.

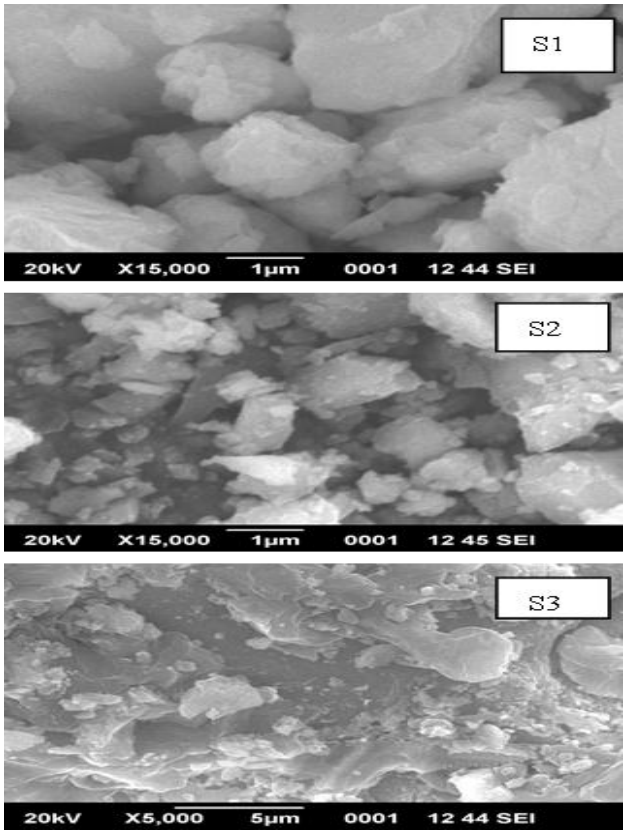

Fig 4. SEM images of S1, S2, S3.

Scanning electron microscopy

The scanning electron microscope (SEM) produces large magnified image, because of the use of electrons rather than light. The SEM has large depth of field, which allows large amount of sample to be in focus at one time. The SEM also produces images of high resolution, which means that closely spaced features can be examined at a high magnification. **Fig. 4** exhibits the typical microstructure FESEM image of as synthesized ZnS powders. The powders exhibited blocky particles with irregular shapes possibly due to the agglomeration of the particles. Agglomeration prevents further disintegration into smaller particles. As the grains are randomly oriented and agglomerated, the actual size of the nanoparticles cannot be determined from the FESEM images **[7].**

Optical absorption

The Absorption spectra of the prepared ZnS nano crystals dispersed in solvent ultrasonically is obtained. Optical spectra of ZnS nanocrystals were recorded in the wavelength range between 200 and 500 nm and these plots are shown in **Fig. 5** as normalized curves. ZnS films have good absorption at short wavelength region, the absorption decreased with increasing wavelength. The increase of the absorption occurs when the photon energy is equal to the value of the energy gap then the electronic transitions between the valance band and the conduction band will begin. However, absorbance in the ultraviolet region is high. The absorption edges are formed at 238nm, 258nm and 280nm for S1, S2 and S3 samples respectively. The enhanced absorption is observed in the neighborhood of 250nm resulting in large quantum confinement effect. It suggests a large blue shift of the absorption edge from that of 320nm (3.73eV) for bulk ZnS crystals at room temperature. Thus, the optical band gap has been enlarged for all the three samples. The extent of energy absorption of a semiconductor is determined by the absorption co-efficient of the material. The optical absorption coefficient α of the film material was obtained from an optical absorbance A using the formula

$$\alpha = 2.303 \times A/t$$

where 't' is the film thickness. A is the absorptance or optical density which is given by

$$A = \log I_o/I$$

where I_o and I being the incident and transmitted intensities of the light, respectively.

The transmitted intensity can be written as $I = I_o \exp(-\alpha)$.

The relation between the absorption coefficient (α) and the energy of incident light (hν) is given by **[14]**,

$$(\alpha h\nu)^n = B(h\nu - E_g)$$

where B is constant and E_g is the optical band gap energy and n = 2 for direct band gap semiconductors. Direct band gap energy E_g, for thin ZnS film was estimated by extrapolating linear portion of the graph of square of $(\alpha h\nu)^2$ against incident photon energy (hν) plots up to the intersection with x-axis **(Fig. 6)**. From the graph, the optical band gap is obtained as 5.2eV, 4.812eV and 4.436eV for S1, S2, and S3 samples respectively.

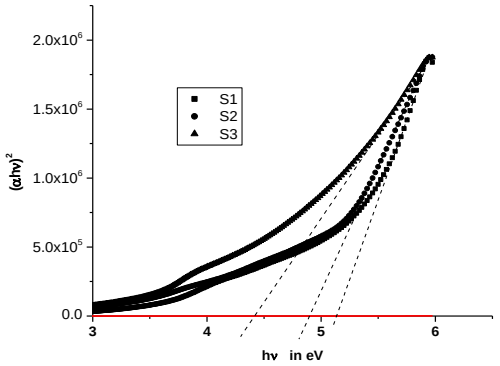

Fig. 5. Optical absorption spectra.

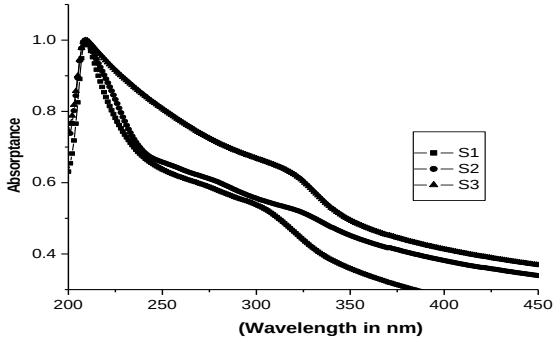

Fig. 6. Graph of $(\alpha h\nu)^2$ Vs hν in eV.

The band gap was increased as sulphur concentration was decreased **(Fig. 7).** This is due to decrease in particle size and large quantum confinement effect. The band gap of 4eV was reported for zinc sulphide material at 0.5M/1M concentration ratio by precipitation method at 80^0C [**4**] which is lesser than the value reported in this paper at the same concentration. Very high band gaps 4.9 to 5.6eV are reported by non-aqueous method at different pH values and synthesized by the same co-precipitation method [**10**]. The band gaps of 3.76 eV, 3.74 eV and 3.65 eV were reported [**13**] at different precursor concentrations of 1:0.7, 1:1 and 1: 1.3 prepared by hydrothermal method at 220^0C, here also the band gap was increased with increase in Zn/S ratio. These values are comparatively lesser than the values reported in this paper which may be due to the different methods and different solvent used for the synthesis. The optical band gap energy in ZnS thin film is decreasing with increasing temperature where SILAR method is used for deposition of films **[5]**. Band gap energy decreased about 110meV with increasing temperature for the temperatures 10 and 320 K, the band gap energy obtained as 3.83 and 3.72 eV respectively. So, compared to SILAR method, in this present work high optical band gap is obtained. Further Using band gap energy, the crystallite size can be calculated using the Brus equation **[2]**

$$\mathbf{E_{g\,(,nano)} = E_{g(bulk)} + \frac{h^2}{8r^2}\ \left[\frac{1}{m_e^*} + \frac{1}{m_h^*}\right] - \frac{1.8e^2}{4\pi\varepsilon\varepsilon_0 r}}$$

Where $E_{g\ (,nano)}$ is the the Energy band gap of the nanomaterial and $E_{g(bulk)}$ is that of bulk material, r is the radius of nanoparticle, m_e^* and m_h^* are the effective masses electron and hole, ε is the dielectric constant of the material. Using m_e^*=0.34 m_e and m_h^*=0.23 m_e and ε =8.3 for ZnS, the crystallite sizes are calculated as 2.68nm, 3.1nm and 3.8nm for the samples S1, S2 and S3 respectively. The difference in the particle size is observed as compared to the values obtained from XRD, this is because of neglecting second term of the brus equation while calculating particle size. The particle sizes of 1.1nm to1.5nm were reported in **[10]** which are calculated using the Brus equation and compared with the values obtained by X Ray Diffraction.

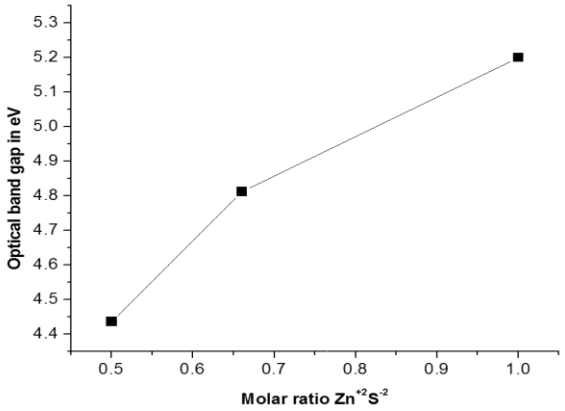

Fig. 7. Graph of molar ratio Vs optical band gap.

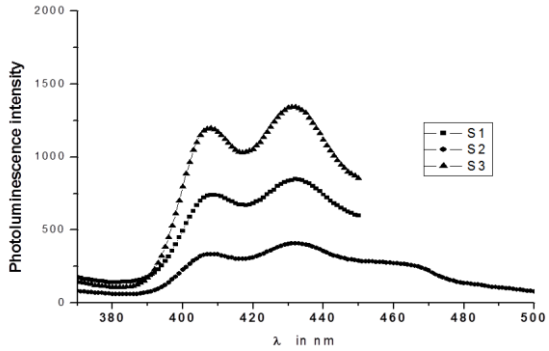

Fig 8. Photoluminescence with peak emissions at 407 and 432nm.

Photoluminescence studies

Photoluminoscence corresponds to the light induced light emission characteristics of the material**.** The **Fig. 8** illustrates the room temp PL spectrum of ZnS nanoparticles as well as Gaussian fitting centered at 328nm obtained at excitation wavelength of 350nm. The Photoluminescence spectra shows resolved two visible violet light emission bands at 407 nm and 432 nm, which are red shifted in the visible range. These emissions might be due to defect energy levels present in the ZnS lattice. This violet emission around 407 nm (3.05 eV) can be attributed to the electron transition from the bottom of the conduction band to the sulphur interstitial level. This transition is positioned at nearly 3.05eV below the CB edge. Whereas the intense violet emission at 432nm is attributed to transition to Zinc vacancy level from the CB. Similar UV emission is investigated by D. Denzler et al **[18]**.

Ellipsometric studies

Optical constants n, k and 't' thickness of the film has been determined using the measured values of psi (Ψ) and Δ (delta) from spectroscopic ellipsometer in the 200-1000nm range. An ellipsometer is an instrument that performs polarization measurements. An unpolarized collimated light beam from a source is first polarized elliptically upon transmission through a polarizer and compensator, is then specularly reflected from the sample, and is finally transmitted through an analyzer before impinging on the detector. The source, polarizer, and compensator (or retarder) work together to generate a state of known polarization before the light beam reaches the sample, whereas the analyzer and detector work together to detect the change in polarization state after the light beam reflects from the sample. A single ellipsometry measurement provides two important interaction parameters, Ψ and Δ at a given wavelength, which can be derived from the polarization state parameters of the beam before and after reflection from the sample. These so-called ellipsometry angles are defined by

$$\tan \Psi \exp(i\Delta) = r_p / r_s,$$

where r_p and r_s are the complex amplitude reflection coefficients of the sample for p and s linear polarization

states, for which the electric field vibrates parallel (p) and perpendicular(s) to the plane of incidence, respectively. The sample parameters n, the real index of refraction, and k, the extinction coefficient can be determined from Ψ and Δ. Due to the phenomenon of dispersion, (n, k) are functions of wavelength and are characteristic of the material from which the sample is composed (often called optical functions).

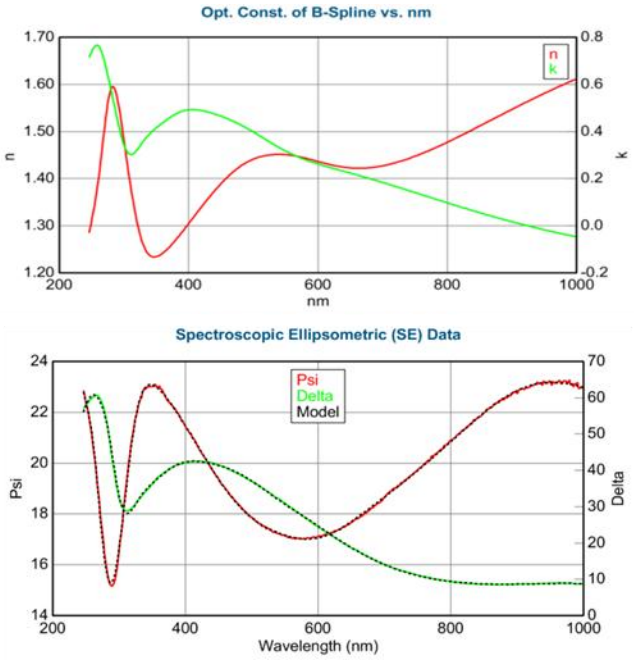

Fig 9. Ellipsometric measurements.

In fact, n and k serve as the real and imaginary parts of the complex index of refraction N=n-ik**.** For the ZnS thin film (S1 sample) prepared by spin coating the refractive index values are varying from 1.3 to 1.6 or it is nearly 1.42578 as established from the ellipsometric measurements in **Fig. 9** at 632.8nm and extinction coefficient k is 0.398 at 500nm and peaks at around 400nm. The thickness of the film is obtained as 528.59nm. This value is used to find the resistivity of the film.

Electrical properties

Conductivity measurements were carried out on the film of sample S1 coated on indium tin oxide glass. Readings were scanned for positive and negative cycles of voltage between -5 to 5V, and corresponding currents were noted. In **Fig. 10** the linear current-voltage plots of these films exhibit ohmic behavior at voltages from -1 to +1 volts upto -5 to +5 volts in the entire measurement range. Current increases linearly for both positive and negative applied bias up to ±5 volts applied. It is clear from these plots that for voltage of 5V, the current in intrinsic film is $6x10^{-4}$A. The bulk resistivity of the film is calculated using the equation ρ = RA/d where ρ is resistivity of the film, A is area of cross section and'd' is the thickness of the film. From the obtained data the minimum resistivity of $2.55x10^{4}$ Ω cm- to $1.242x10^{3}$ Ω cm is noted which is less than the values reported in Ref. **[18].** The resistivity of 1.69 x 10^{4} Ω cm is reported in ref. **[17]** for the films ann ealed at 400°C and $1.73x10^{4}$ Ω cm for as deposited films. In case of ZnS thin films prepared by SILAR method **[5],** I– V behaviour for as-grown and annealed films at 100,150, 200 and 250 ^{0}C temperature and light effect on I–V behaviour of films was investigated. The current values are about 10^{-10}A, which is less than the current values reported in this paper and this is due to lower optical band gap of ZnS thin films.

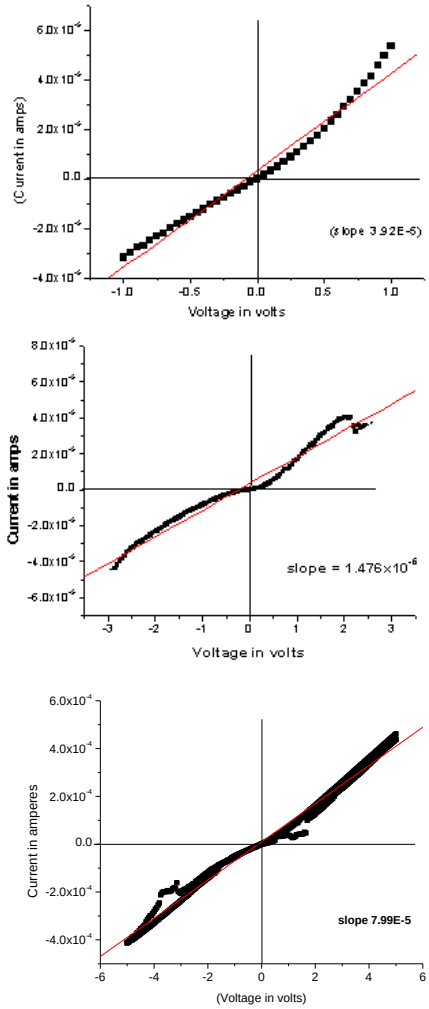

Fig. 10. VI charectaristics of ZnS thin film (S1).

Conclusions

ZnS has great potential as a useful material for nanoscale devices due to its non-toxicity and wider band gap as compared to Cadmium Sulphide (CdS) buffer layers. They offer the opportunity to create structures with unique properties, such as tunable optical performance. In this work, ZnS nano crystals are synthesized by simple co-precipitation method using low cost precursors without using any capping agent at different precursor concentrations. As prepared samples are analysed by

X-ray diffraction, SEM, EDS and UV-Vis spectrophotometry. The effect of sulphur concentration on structural and optical properties were studied. Metal to sulphide ratio have been shown to have a significant effect on the amount of zinc ions precipitated from solution and hence on the particle size. X ray diffraction reveals crystalline nature of material with cubic phase and particles of 4.92nm, 8.56 and 11nm were formed. The optical absorption studies reveal a large blue shift of the absorption edge from their bulk values resulting in quantum confinement effect. The optical band gap is decreased as the sulphur concentration in the reaction mixture was increased. This will be useful for exploring various applications of ZnS based optical and optoelectronic devices.

Acknowledgements

This work has been supported by Research and Development cell, B.V.B.College of Engineering and Technology, Hubballi under Capacity building projects. The authors are thankful to Dr.M.K.Rebinal, Department of Physics, Karnataka University Dharwad and HOD, Dept of Chemistry B.V.B.College of Engineering and Technology, and Center for Materials Research, Hubballi for providing Laboratory facilities.

References

1. *Ummartyotin, S.; Infahsaeng, Y; Renewable Sustainable Energy Rev.,2016,55,17*
DOI: 10.1016/j.rser.2015.10.120.
2. Konstantatos,G,; Sargent,E.H,; (Edi. I),; Colloidal Quantum Dot Optoelectronics and Photovoltaics; Cambridge University Press, UK,2013.
3. Fang, X.; Zhai,T,; Gautam,U.K,; Li,L.; Wua,L; Bando,Y; Golberg.D; Prog. Mater. Sci.*; 2011,56, 175,*
DOI:10.1016/j.rser.2015.10.120
4. *Fang, X.; Bando,Y; Gautam,U.K,; Zhai,T,; Zeng,H.; Xu,X.; Liao,M.; Golberg,D; CRC Crit. Rev. Solid State Sci.; 2009,34,190.*
DOI: 10.1080/10408430903245393
5. Ates,M.; Ali Yıldırım,M.; Kundakcı,M.; Astam,A.; Mater. Sci. Semicond. Process.; 2007,10,281,
DOI: 10.1016/j.mssp.2008.04.003
6. *Gangopadhyay,U.; Kim,K.; Mangalaraj, D.; Yi,J.; Appl. Surf. Sci.*, 2004**,** 230, 364
DOI: 10.1016/j.apsusc.2004.02.059
7. *Bindu,K.R.; Sreenivasan,P.V.; Mortinez,A.I.; Anila, E.I.;, J. Sol-Gel Sci. Technol.,2013,68, 351*
DOI: 10.1007/s10971-013-3177-4
8. *Ummartyotin, S.; Bunnak,N.; Juntaro, J.; Sain,M.; Manuspiya,H.; Solid State Sci., 2012,14, 299*
DOI: http://dx.doi.org/10.1016/j.solidstatesciences.2011.12.005
9. Goktas,A.; Aslan,F.; Yasar,E.; Mutlu,I.H.; J. Mater. Sci.: Mater. Electron.,2012,23,1361.
DOI: 10.1007/s10854-011-0599-z
10. Firoozifar, S.A.R.;, Behjata, A.; Kadivar, E.; Ghorashia, S.M.B.; Zarandia, M. B. ; *Appl. Surf. Sci.*, **2011,** 258 , 818
DOI: 10.1016/j.apsusc.2011.08.105
11. Tec-Yam,S.; Rojas,J,; Rejón,V.; Oliva,A.; Mater. Chem. Phys.,2012,136,386
DOI: 10.1016/j.matchemphys.2012.06.063
12. Yoo,D.; Choi,M.K.; Heo,S.C.; Chung,C.;Kim,D.;Choi,C.; Met. Mater. Int. , 2013,19,1309
DOI: 10.1007/s12540-013-6026-7
13. Kole,A.K.; Kumbhakar,P.; Results Phys., 2012,2,150.
DOI: http://dx.doi.org/10.1016/j.rinp.2012.09.010
14. Saleem,M.; Fang,L.; Wakeel,A.; Rashad,M.; Kong,C.Y.;World J. Condens. Matter Phys.,2012, 2,10
DOI: 10.4236/wjcmp.2012.21002
15. Lewis,A.E.; *Hydrometallurgy*, 2010,104, 222
DOI: 10.1016/j.hydromet.2010.06.010
16. Hoa,T.T.Q.; Vu,L.V.;Canh,T.D.;Long,N.N.; J. Phys.: Conf. Ser., 2009
DOI: 10.1088/1742-6596/187/1/012081
17. Haque, F.; Rahman, A.S.; Islam, M.A.; Rashid, M.J.; Akhtaruzzaman, M.; Alam, M.M.; Alothman, Z.A.; Sopian, K.; Amin, N.; Chalcogenide Lett., 2014 ,11, 189
DOI: chalcogen.ro/189_Haque.pdf
18. Denzler, D.; Olschewski, M.; Sattler, K.; J. Appl. Phys.,1998, 84,2481.
DOI: http://dx.doi.org/10.1063/1.368425

